

# Baryon Octet Electromagnetic Form Factors in a confining NJL model

Manuel E. Carrillo-Serrano,<sup>1</sup> Wolfgang Bentz,<sup>2</sup> Ian C. Cloët,<sup>3</sup> and Anthony W. Thomas<sup>1</sup>

<sup>1</sup>*CSSM and ARC Centre of Excellence for Particle Physics at the Tera-scale,  
Department of Physics, University of Adelaide, Adelaide SA 5005, Australia*

<sup>2</sup>*Department of Physics, School of Science, Tokai University, Hiratsuka-shi, Kanagawa 259-1292, Japan*

<sup>3</sup>*Physics Division, Argonne National Laboratory, Argonne, Illinois 60439, USA*

Electromagnetic form factors of the baryon octet are studied using a Nambu–Jona-Lasinio model which utilizes the proper-time regularization scheme to simulate aspects of colour confinement. In addition, the model also incorporates corrections to the dressed quarks from vector meson correlations in the  $t$ -channel and the pion cloud. Comparison with recent chiral extrapolations of lattice QCD results shows a remarkable level of consistency. For the charge radii we find the surprising result that  $r_E^p < r_E^{\Sigma^+}$  and  $|r_E^n| < |r_E^{\Xi^0}|$ , whereas the magnetic radii have a pattern largely consistent with a naive expectation based on the dressed quark masses.

PACS numbers: 12.39.Fe, 13.40.Gp, 14.20.-c

Keywords: baryon octet, electromagnetic form factors

## I. INTRODUCTION

The lowest mass baryon octet plays a special role in the quest to understand the strong interaction. Along with their masses and axial charges, it is particularly important to explain their distributions of charge and magnetisation in terms of the underlying quark-gluon dynamics. Empirically, these distributions are expressed by their electromagnetic form factors, which present an extraordinary challenge for QCD [1]. Considerable experimental effort has been devoted to the measurement and parametrization of the electromagnetic form factors of the nucleon [2–13]. However, for the other members of the baryon octet this is a more difficult task because of their short lifetimes [14].

Theoretical predictions for nucleon electromagnetic form factors, and for example, parton distribution functions, have been made using a variety of approaches, such as quark models [15–26], QCD sum rules [27], the Dyson-Schwinger equations [28–30] and lattice QCD simulations [31–39]. For the other elements of the octet, prior to lattice QCD computations, early work on the spectrum, electromagnetic form factors and weak form factors was based on, for example, the bag model [40–51], QCD sum rules [27], constituent quark models [52–54] and more recently the Dyson-Schwinger equations [55].

With the advent of more precise lattice QCD computations, together with chiral extrapolations to the physical point, the baryon octet spectrum has been accurately reproduced [32, 35, 56] and more recently the electromagnetic form factors of the outer ring of the octet have been extracted [38, 39]. At the same time, the recent work in Ref. [26] showed promising results when the Nambu–Jona-Lasinio (NJL) model [57, 58] was applied to the calculation of the nucleon electromagnetic form factors [26]. In addition, the model has also been applied to the axial charges in several  $\Delta S = 0$   $\beta$ -decays in the baryon octet [54], and the electromagnetic form factors of the  $\rho$  meson [59].

In the present work we extend the framework developed in Ref. [26] for the nucleon, to a description of the electromagnetic form factors of the baryon octet.

## II. BARYONS IN A NAMBU–JONA-LASINIO MODEL

Extensive reviews of the NJL model exist [61, 62, 67] and here we use the  $SU(3)$  flavour version with only the four-fermion interaction. The Lagrangian in the  $q\bar{q}$  interaction channel, which we take in Fierz symmetric form [61], reads

$$\mathcal{L} = \bar{\psi} (i\cancel{\partial} - \hat{m}) \psi + \frac{1}{2} G_\pi \left[ (\bar{\psi} \lambda_i \psi)^2 - (\bar{\psi} \gamma_5 \lambda_i \psi)^2 \right] - \frac{1}{2} G_\rho \left[ (\bar{\psi} \gamma^\mu \lambda_i \psi)^2 + (\bar{\psi} \gamma^\mu \gamma_5 \lambda_i \psi)^2 \right], \quad (1)$$

with  $\hat{m} = \text{diag} [m_u, m_d, m_s]$  and  $\lambda_i$  the eight Gell-Mann matrices plus  $\lambda_0 \equiv \sqrt{2/3} \mathbb{1}$ . Gluon degrees of freedom are absent in the NJL model and therefore one must specify a method of regularization. We use the proper-time scheme, because it simulates aspects of quark confinement [63–65].

The dressed quark mass,  $M_q$ , of flavour  $q = u, d, s$  is obtained by solving the gap equation. With proper-time regularization  $M_q$  satisfies [54]

$$M_q = m_q + \frac{3}{\pi^2} M_q G_\pi \int_{1/\Lambda_{UV}^2}^{1/\Lambda_{IR}^2} d\tau \frac{e^{-\tau M_q^2}}{\tau^2}. \quad (2)$$

We note that in the  $SU(3)$  flavour case, flavour mixing is absent, in contrast to the  $SU(2)$  flavour case [61].

When solving the 3-body problem [66] in the NJL model, to obtain the Faddeev vertex functions for each member of the baryon octet, strong diquark correlations naturally appear. To determine the diquark  $t$ -matrices it is therefore convenient to make a different Fierz transformation on the  $SU(3)$  NJL Lagrangian density, which yields the effective  $qq$  interactions [68] in the scalar and

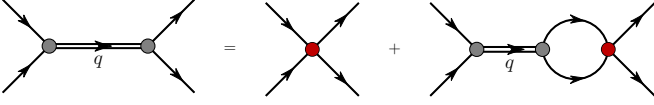


Figure 1. (Colour online) Inhomogeneous Bethe-Salpeter equation for quark–quark (diquark) correlations.

axial-vector diquark channels:

$$\begin{aligned} \mathcal{L}_I^{qq} &= G_s \left[ \bar{\psi} \gamma_5 C \lambda_a \beta_A \psi^T \right] \left[ \psi^T C^{-1} \gamma_5 \lambda_a \beta_A \psi \right] \\ &+ G_a \left[ \bar{\psi} \gamma_\mu C \lambda_s \beta_A \psi^T \right] \left[ \psi^T C^{-1} \gamma^\mu \lambda_s \beta_A \psi \right], \quad (3) \end{aligned}$$

where  $C = i\gamma_2\gamma_0$  is the charge conjugation matrix, and  $G_s$  and  $G_a$  are the couplings in the scalar and axial-vector diquark channels, respectively. The quark flavour matrices are represented by  $\lambda_a$  for  $a \in (2, 5, 7)$  and  $\lambda_s$  for  $s \in (0, 1, 3, 4, 6, 8)$ , while  $\beta_A = \sqrt{3/2} \lambda_A$  ( $A = 2, 5, 7$ ) selects the colour  $\bar{3}$  states [68–70].

Fig. 1 depicts the Bethe-Salpeter equation (BSE) which describes two-particle ( $qq$  in this case) bound states. Solutions to the BSE for the scalar and axial-vector diquarks, in terms of the reduced  $t$ -matrices, are expressed as

$$\tau_{[q_1 q_2]}(q) = \frac{4i G_s}{1 + 2 G_s \Pi_{[q_1 q_2]}(q^2)}, \quad (4)$$

$$\begin{aligned} \tau_{\{q_1 q_2\}}^{\mu\nu}(q) &= \frac{4i G_a}{1 + 2 G_a \Pi_{\{q_1 q_2\}}^T(q^2)} \left( g^{\mu\nu} - \frac{q^\mu q^\nu}{q^2} \right) \\ &+ \frac{4i G_a}{1 + 2 G_a \Pi_{\{q_1 q_2\}}^L(q^2)} \frac{q^\mu q^\nu}{q^2}. \quad (5) \end{aligned}$$

The bubble diagrams are given by

$$\Pi_{[q_1 q_2]}(q^2) = 6i \int \frac{d^4 k}{(2\pi)^4} \text{Tr} [\gamma_5 S_{q_1}(k) \gamma_5 S_{q_2}(k+q)], \quad (6)$$

$$\begin{aligned} \Pi_{\{q_1 q_2\}}^T(q^2) \left( g^{\mu\nu} - \frac{q^\mu q^\nu}{q^2} \right) + \Pi_{\{q_1 q_2\}}^L \frac{q^\mu q^\nu}{q^2} &= \\ 6i \int \frac{d^4 k}{(2\pi)^4} \text{Tr} [\gamma^\mu S_{q_1}(k) \gamma^\nu S_{q_2}(k+q)], \quad (7) \end{aligned}$$

where  $S_q(k) = [\not{k} - M_q + i\varepsilon]^{-1}$  is the dressed quark propagator and the trace is over Dirac indices only. Throughout this paper square brackets will represent a scalar diquark and curly brackets an axial-vector diquark, where  $q_1$  and  $q_2$  label the flavour ( $u, d, s$ ) of each quark inside the diquark. In the solution to the Faddeev equation we employ the pole approximation for the reduced  $t$ -matrices [26, 54]:

$$\tau_{[q_1 q_2]}(q) \rightarrow \frac{-i Z_{[q_1 q_2]}}{q^2 - M_{[q_1 q_2]}^2 + i\varepsilon}, \quad (8)$$

$$\tau_{\{q_1 q_2\}}^{\mu\nu}(q) \rightarrow \frac{-i Z_{\{q_1 q_2\}}}{q^2 - M_{\{q_1 q_2\}}^2 + i\varepsilon} \left( g^{\mu\nu} - \frac{q^\mu q^\nu}{M_{\{q_1 q_2\}}^2} \right). \quad (9)$$

where the  $Z$ 's are the residues at the poles [26, 54].

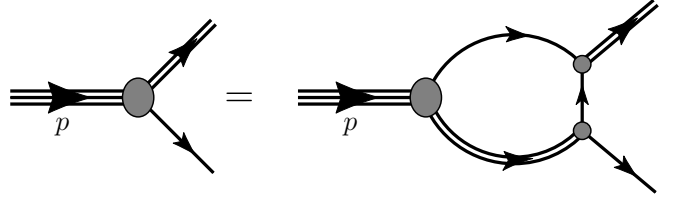


Figure 2. Homogeneous Poincaré covariant Faddeev equation whose solution gives the mass and vertex function for each member of the baryon octet.

Solutions to the Faddeev equation for each member of the baryon octet in this model have already been detailed in Ref. [54], therefore here we will just give a brief review. For each baryon the Faddeev equation, in the static approximation [71], takes the general form

$$\Gamma_b(p, s) = Z_b \Pi_b(p) \Gamma_b(p, s), \quad (10)$$

where  $b = N, \Sigma, \Xi$  labels the baryon and the  $p^2$  that satisfies this equation defines the baryon mass. The quark exchange kernel is labelled by  $Z_b$  and  $\Pi_b(p)$  contains the quark–diquark bubble diagrams. The Faddeev vertex is normalized such that  $\Gamma_b(p, s) = \sqrt{-Z_b} \Gamma_{0b}(p, s)$ , where  $Z_b$  is given by

$$Z_b^{-1} = \bar{\Gamma}_{0b} \frac{\partial \Pi_b(p)}{\partial \not{p}} \Gamma_{0b} \Big|_{p^2=M_b^2}. \quad (11)$$

We normalize the vertex  $\Gamma_{0b}(p, s)$  such that  $\bar{\Gamma}_{0b} \Gamma_{0b} = 1$ .

For the form factor calculations we will only consider the nucleon,  $\Sigma^\pm$  and  $\Xi$ , as there are no lattice results for the  $\Lambda$  and the  $\Sigma^0$ . The Faddeev vertex functions are evaluated for equal light quark masses ( $M_u = M_d \equiv M_\ell$ ) and for the members of the baryon octet considered, the Dirac structure is

$$\begin{aligned} \Gamma_b(p, s) &= \begin{bmatrix} \Gamma_{q_1 [q_1 q_2]}(p, s) \\ \Gamma_{q_1 \{q_1 q_2\}}^\mu(p, s) \\ \Gamma_{q_2 \{q_1 q_1\}}^\mu(p, s) \end{bmatrix}, \\ &= \sqrt{-Z_b} \begin{bmatrix} \alpha_1 \\ \alpha_2 \frac{p^\mu}{M_b} \gamma_5 + \alpha_3 \gamma^\mu \gamma_5 \\ \alpha_4 \frac{p^\mu}{M_b} \gamma_5 + \alpha_5 \gamma^\mu \gamma_5 \end{bmatrix} u_b(p, s). \quad (12) \end{aligned}$$

The quark exchange kernel reads

$$Z_b = 3 \begin{bmatrix} \frac{1}{M_{q_1}} & \frac{1}{M_{q_1}} \gamma_\sigma \gamma_5 & -\frac{\sqrt{2}}{M_{q_2}} \gamma_\sigma \gamma_5 \\ \frac{1}{M_{q_1}} \gamma_5 \gamma_\mu & \frac{1}{M_{q_1}} \gamma_\sigma \gamma_\mu & \frac{\sqrt{2}}{M_{q_2}} \gamma_\sigma \gamma_\mu \\ -\frac{\sqrt{2}}{M_{q_2}} \gamma_5 \gamma_\mu & \frac{\sqrt{2}}{M_{q_2}} \gamma_\sigma \gamma_\mu & 0 \end{bmatrix}, \quad (13)$$

where, following Ref. [54],  $M_{q_1}$  and  $M_{q_2}$  correspond to the masses of the singly and doubly represented quark, respectively. Projecting the Faddeev kernel onto a colour singlet gives the factor of 3 in Eq. (13).

The parameters employed here are summarized in Tab. I. The infrared cutoff should be of the order of

$\Lambda_{IR}$	$\Lambda_{UV}$	$M_\ell$	$M_s$	$G_\pi$	$G_\rho$	$G_s$	$G_a$
0.240	0.645	0.40	0.56	19.0	11.0	5.8	4.9

Table I. Model parameters, where all masses and regularization parameters are given in units of GeV, while the Lagrangian couplings are in units of  $\text{GeV}^{-2}$ .

$M_{[\ell\ell]}$	$M_{[\ell s]}$	$M_{\{\ell\ell\}}$	$M_{\{\ell s\}}$	$M_{\{ss\}}$	$Z_{[\ell\ell]}$	$Z_{[\ell s]}$	$Z_{\{\ell\ell\}}$	$Z_{\{\ell s\}}$	$Z_{\{ss\}}$
0.768	0.903	0.929	1.04	1.15	11.1	12.0	6.73	7.54	8.36

Table II. Results for the diquark masses and pole residues in the various diquark  $t$ -matrices [c.f. Eqs. (8) and (9)]. All masses are in GeV and the residues are dimensionless.

$\Lambda_{\text{QCD}}$  because it implements quark confinement [64, 65], and we choose  $\Lambda_{IR} = 0.240$  GeV. The masses of the light dressed quarks are chosen as  $M_u = M_d = M_\ell = 0.4$  GeV, while the  $s$ -quark mass,  $M_s$ , is chosen to reproduce the mass of the  $\Omega^-$  baryon. The parameters  $\Lambda_{UV}$ ,  $G_\pi$  and  $G_\rho$  are fit to reproduce the empirical values of the pion decay constant, and the pion and  $\rho$  masses, while  $G_a$  and  $G_s$  are fixed by the physical  $\Delta^{++}$  and nucleon masses.

In Tab. II we summarize the results for the diquark masses, as well as the residues for the diquark  $t$ -matrices given in Eqs. (8) and (9). The octet baryon masses, obtained by solving the appropriate Faddeev equation, are given in Tab. III. The parameters defining the Faddeev vertex function for each member of the baryon octet are summarized in Tab. IV.

### III. BARYON FORM FACTORS

The electromagnetic form factors,  $F_{1b}$  and  $F_{2b}$ , of an octet baryon  $b$ , are defined by the electromagnetic current

$$j_{\lambda'\lambda}^{\mu,b}(p', p) = \langle p', \lambda' | J_{em}^\mu | p, \lambda \rangle, \quad (14)$$

$$= \bar{u}_b(p', \lambda') \left[ \gamma^\mu F_{1b}(Q^2) + \frac{i\sigma^{\mu\nu} q_\nu}{2M_b} F_{2b}(Q^2) \right] u_b(p, \lambda),$$

where  $\lambda$  and  $\lambda'$  represent the helicity of the incoming and outgoing baryon and  $q$  is the 4-momentum transfer, where  $Q^2 = -q^2$ . In the NJL model considered here, this electromagnetic current is represented by the Feynman diagrams illustrated in Fig. 3.

In the evaluation of the baryon form factors we dress the quark-photon vertices by including both vector meson correlations in the  $t$ -channel, through the inhomogeneous BSE, and also effects from pion loops. This formalism is described in detail in Ref. [26]. In summary, the dressed quark-photon vertex has the form:

$$\Lambda_{\gamma Q}^\mu(p', p) = \gamma^\mu F_{1Q}(Q^2) + \frac{i\sigma^{\mu\nu} q_\nu}{2M_q} F_{2Q}(Q^2), \quad (15)$$

where  $Q = (U, D, S)$  and the  $F_{2Q}$  form factor results from the pion loop corrections. Explicit expressions for the dressed quark form factors can be found in Ref. [26],

	$M_N$	$M_\Lambda$	$M_\Sigma$	$M_\Xi$
NJL	0.940	1.126	1.170	1.277
Experiment	0.940	1.116	1.193	1.318

Table III. Calculated octet baryon masses are compared with the average experimental mass for the corresponding multiplet. Note that the nucleon mass was used to constrain an NJL model parameter. All masses are in units of GeV.

	$\alpha_1$	$\alpha_2$	$\alpha_3$	$\alpha_4$	$\alpha_5$	$Z_B$
nucleon	0.552	0.031	-0.233	-0.043	0.329	28.136
$\Sigma$	0.506	0.066	-0.211	-0.051	0.352	20.041
$\Xi$	0.525	0.046	-0.249	-0.044	0.324	18.819

Table IV. Coefficients that define the Faddeev vertex functions for each member of the baryon octet considered herein.

supplemented here with the dressed strange quark form factors:  $F_{1S} = -\frac{1}{3}F_{1\phi}$  and  $F_{2S} = 0$ , where  $F_{1\phi}$  is generated by  $t$ -channel  $\phi$  meson correlations [26]. Because the  $\pi$  is much lighter than the  $K$  we expect pion loops to give the dominant chiral correction, and therefore omit  $K$  loops [60].

The total baryon form factors have the form

$$F_{ib}(Q^2) = \sum_Q \left[ F_{1Q} f_{ib}^{Q,V} + F_{2Q} f_{ib}^{Q,T} \right], \quad (16)$$

where the sum is over the dressed quarks in each baryon and the  $Q^2$  dependence for each form factor is implicit. The body form factors,  $f_{ib}^{Q,V}$  and  $f_{ib}^{Q,T}$ , are given by the Feynman diagrams of Fig. 3, where the former is obtained from a point-like quark-photon vector coupling  $\gamma^\mu$  and the latter a point-like quark-photon tensor coupling  $i\sigma^{\mu\nu} q_\nu / 2M_q$ . Each of these body form factors contains contributions from both the quark and diquark diagrams illustrated in Fig. 3, and further details can be found in Refs. [26, 54]

The Sachs form factors are defined by

$$G_{Eb} = F_{1b} - \frac{Q^2}{4M_b^2} F_{2b}, \quad G_{Mb} = F_{1b} + F_{2b}, \quad (17)$$

and in Tab. V results for  $G_{Mb}$  at  $Q^2 = 0$  are given, with both the vector meson dressing of the quark-photon vertices (labelled BSE) and also with the effect of the pion

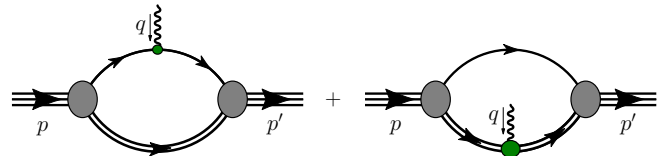


Figure 3. (Colour online) Feynman diagrams representing the electromagnetic current for the octet baryons. The diagram on the left is called the “quark diagram” and the one on the right the “diquark diagram”. In the diquark diagram the photon interacts with each quark inside the diquark.

	$\mu_b^{(BSE)}$	$\mu_b$	$\mu_b^{exp}$
proton	2.43	2.78	2.793
neutron	-1.25	-1.81	-1.913
$\Sigma^+$	2.30	2.62	2.458(10)
$\Sigma^-$	-1.04	-1.62	-1.160(25)
$\Xi^0$	-1.08	-1.14	-1.250(14)
$\Xi^-$	-0.78	-0.67	-0.6507(25)

Table V. Magnetic moments in units of nuclear magnetons. The BSE results include only the vector meson contributions to the dressed quark form factors, while the final results also include effects from the pion cloud. A comparison with the experimental values [14] is shown.

cloud as well. It is evident that the effect of the pion cloud is to increase the magnitude of the magnetic moments across the octet, almost uniformly improving agreement with experiment. The exception is the  $\Sigma^-$ , where the discrepancy is about 40%, which suggests that in this case the effect of the pion cloud may be overestimated [49, 50].

Results for the charge and magnetic radii of the octet baryons, defined with respect to the Sachs form factors, are summarized in Tab. VI. The PL column stands for a structureless, point-like quark and the other two columns use either the BSE or the fully dressed quark-photon vertex. The effect of the vector meson and pion cloud dressing on these quantities is evident. In all cases the radii increase with the inclusion of vector meson corrections, sometimes dramatically. The effect of the pion cloud alone is also to increase the radii, except for the  $\Xi^-$ , where  $r_M^{\Xi^-}$  is reduced from 0.62 fm with only the BSE vertex to 0.51 fm including the pion cloud. The maximum contribution appears in the neutron charge radius where we find an increase of 85% from the pion cloud alone. The smallest contribution of the pion cloud occurs for the magnetic radius of the  $\Xi^0$  and  $\Xi^-$ , which is to be expected because the strange quarks do not couple to the pion cloud.

Surprisingly, we find that  $r_E^p < r_E^{\Sigma^+}$  and  $|r_E^n| < |r_E^{\Xi^0}|$ . This is because the difference between  $m_{\rho(\omega)}$  and  $m_\phi$  (about 250 MeV), which characterize the vector meson dressing of the quark-photon vertices, makes the slope of  $F_{1D}$  at  $Q^2 = 0$  around 1.78 times larger than that for  $F_{1S}$  in the BSE case, and 2.45 times larger including the pion cloud. The contributions from these form factors tend to lower the charge radius, suppressing  $r_E$  more in the nucleon than in the  $\Sigma^+$  or  $\Xi^0$ . In addition, for the proton the term arising from the  $F_{2D}$  form factor reduces the proton radius even further, and this term is absent in the  $\Sigma^+$  because the strange quark does not couple to the pion field.

Our main results, presented in Fig. 4, compare the octet form factors calculated here with those obtained in Ref. [38, 39] via chiral extrapolation of lattice QCD simulations (on two different volumes) to the physical quark masses. For the magnetic form factors of the neutron,  $\Sigma^-$  and  $\Xi^-$  it is evident the contribution from the

	$r_E^{(PL)}$	$r_E^{(BSE)}$	$r_E$	$r_M^{(PL)}$	$r_M^{(BSE)}$	$r_M$
proton	0.51	0.81	0.87	0.43	0.76	0.87
neutron	-0.19	-0.20	-0.37	0.39	0.74	0.91
$\Sigma^+$	0.53	0.85	0.96	0.45	0.76	0.88
$\Sigma^-$	0.46	0.74	0.86	0.48	0.80	0.96
$\Xi^0$	0.17	0.37	0.49	0.35	0.62	0.66
$\Xi^-$	0.44	0.69	0.76	0.42	0.62	0.51

Table VI. Electric and magnetic radii (in fm). PL stands for a point-like quark, BSE includes only the vector meson contributions to the dressed quark form factors, and the final results include both BSE and the effect of the pion cloud.

pion cloud is significant, primarily at low  $Q^2$ . The effect of the pion cloud on the nucleon electric form factors appears to improve the agreement with the lattice simulations (which are in quite good agreement with the empirical data), whereas the magnetic form factors are still underestimated.

The other members of the octet appear to have a similar behaviour. However, for the  $\Sigma^-$  the curvature of  $G_M$  is dramatically increased by the pion cloud. This behaviour matches the large increase of the  $\Sigma^-$  magnetic moment reported earlier.  $G_E^{\Sigma^-}$  is consistent with the lattice results within the same level of accuracy found for the nucleon,  $\Sigma^+$  and  $\Xi^0$ . Finally,  $G_M^{\Xi^-}$  shows outstanding agreement with the lattice data but  $G_E^{\Xi^-}$  is above the data, just as found for the other members of the octet.

The possible explanation of these small, but non-negligible differences could well be a consequence of the fact that there are still systematic errors from the lattice simulation and the chiral extrapolation technique.

#### IV. CONCLUSIONS

We have presented a study of the electromagnetic form factors of the baryon octet over an extended range of momentum transfer. The calculations were made within the NJL model, using proper-time regularization to simulate confinement and included dressing at the quark-photon vertices from vector mesons and pion loops. This work was stimulated by the recent lattice QCD calculations of these quantities, which presented results (after chiral extrapolation) at a discrete set of values of  $Q^2$  up to 1.4 GeV<sup>2</sup>. In comparing the model calculations with these lattice results one must bear in mind that there may still be systematic errors at the level of 10% arising from lattice artifacts as well as the chiral extrapolation.

Overall, the level of agreement between the model calculations and the lattice results is qualitatively impressive. We expect that the results presented here will stimulate calculations in other approaches and trust that the comparison between those results, future lattice calculations and the results presented here will indeed lead to important new insights into hadron structure.

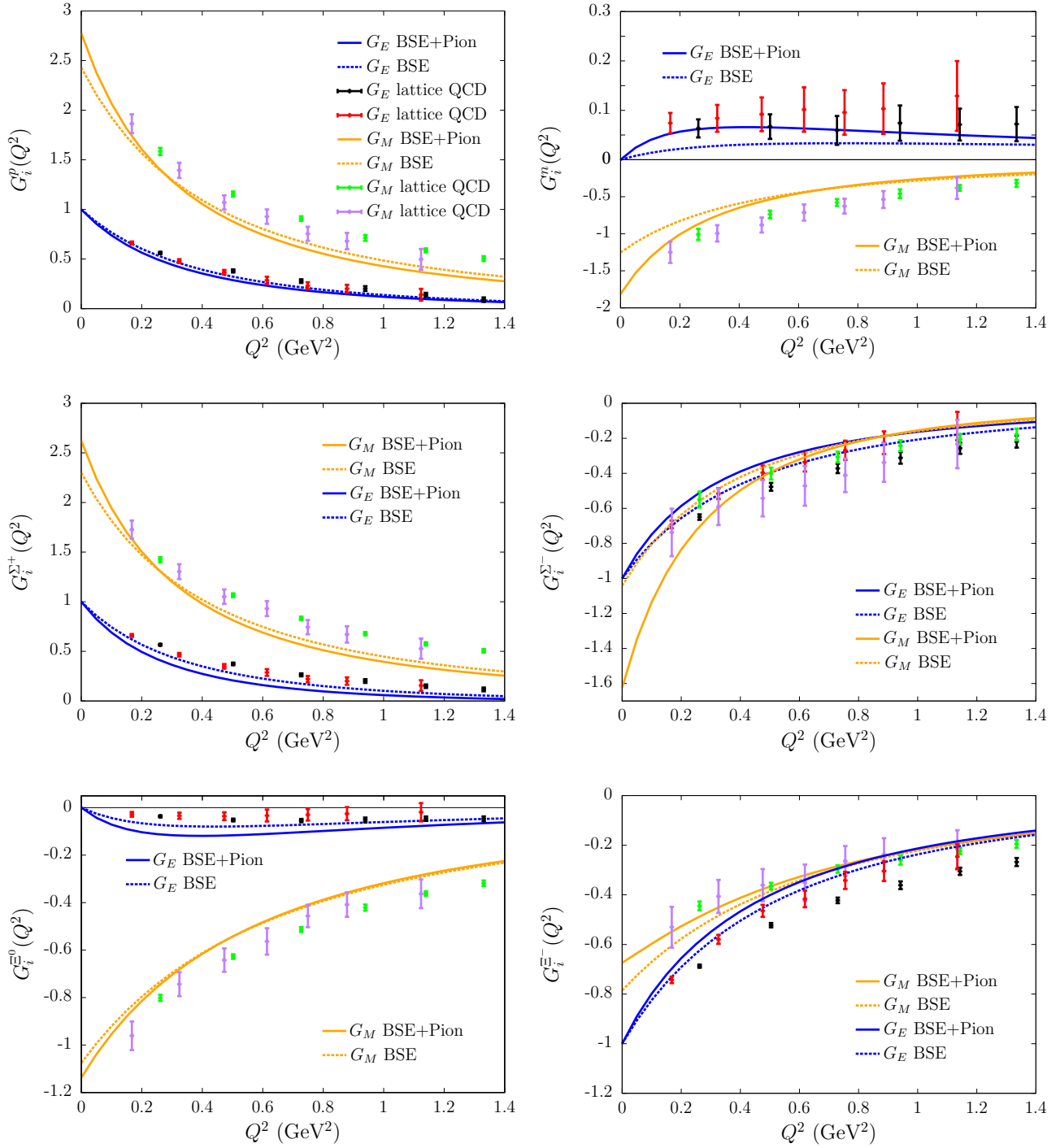


Figure 4. (Colour online) Electromagnetic form factors of the octet baryons with  $i = (E, M)$  indicating the Sachs electric and magnetic form factors. The plots show results from the vector meson dressing contributions to the quark-photon vertex (BSE) and the case where the pion cloud also included (BSE+Pion). In all the plots the points with error bars correspond to the chiral extrapolation of lattice results presented in Ref. [38, 39], which are based on two different lattice volumes. In each case the magnetic form factors are normalized such that the value at  $Q^2 = 0$  represents the baryon magnetic moment in units of nuclear magnetons.

## ACKNOWLEDGEMENTS

This material is based upon work supported by the U.S. Department of Energy, Office of Science, Office of Nuclear Physics, under contract number DE-AC02-06CH11357; the Australian Research Council through the ARC Cen-

tre of Excellence in Particle Physics at the Terascale, an ARC Australian Laureate Fellowship FL0992247 and DP151103101; and the Grant in Aid for Scientific Research (Kakenhi) of the Japanese Ministry of Education, Sports, Science and Technology, Project No. 25400270.

- 
- [1] J. Arrington, C. D. Roberts and J. M. Zanotti, *J. Phys. G* **34**, S23 (2007) [nucl-th/0611050].
- [2] S. J. Brodsky and G. R. Farrar, *Phys. Rev. Lett.* **31**, 1153 (1973).
- [3] S. J. Brodsky and G. R. Farrar, *Phys. Rev. D* **11**, 1309 (1975).
- [4] G. R. Farrar and D. R. Jackson, *Phys. Rev. Lett.* **43**, 246 (1979).
- [5] V. Tadevosyan *et al.* [Jefferson Lab F(pi) Collaboration], *Phys. Rev. C* **75**, 055205 (2007) [nucl-ex/0607007].
- [6] M. K. Jones *et al.* [Jefferson Lab Hall A Collaboration], *Phys. Rev. Lett.* **84**, 1398 (2000) [nucl-ex/9910005].
- [7] O. Gayou, K. Wijesooriya, A. Afanasev, M. Amarian, K. Aniol, S. Becher, K. Benslama and L. Bimbot *et al.*, *Phys. Rev. C* **64**, 038202 (2001).
- [8] O. Gayou *et al.* [Jefferson Lab Hall A Collaboration], *Phys. Rev. Lett.* **88**, 092301 (2002) [nucl-ex/0111010].
- [9] J. P. Ralston and P. Jain, *Phys. Rev. D* **69**, 053008 (2004) [hep-ph/0302043].
- [10] J. J. Kelly, *Phys. Rev. C* **70**, 068202 (2004).
- [11] C. F. Perdrisat, V. Punjabi and M. Vanderhaeghen, *Prog. Part. Nucl. Phys.* **59**, 694 (2007) [hep-ph/0612014].
- [12] J. C. Bernauer *et al.* [A1 Collaboration], *Phys. Rev. Lett.* **105**, 242001 (2010) [arXiv:1007.5076 [nucl-ex]].
- [13] A. J. R. Puckett, E. J. Brash, O. Gayou, M. K. Jones, L. Pentchev, C. F. Perdrisat, V. Punjabi and K. A. Aniol *et al.*, *Phys. Rev. C* **85**, 045203 (2012) [arXiv:1102.5737 [nucl-ex]].
- [14] K. A. Olive *et al.* [Particle Data Group Collaboration], *Chin. Phys. C* **38**, 090001 (2014).
- [15] A. Le Yaouanc, L. Oliver, O. Pene and J. -C. Raynal, *Phys. Rev. D* **18**, 1591 (1978).
- [16] N. Isgur and G. Karl, *Phys. Rev. D* **20**, 1191 (1979).
- [17] A. W. Thomas, S. Theberge and G. A. Miller, *Phys. Rev. D* **24**, 216 (1981).
- [18] D. Diakonov, V. Petrov, P. Pobylitsa, M. V. Polyakov and C. Weiss, *Nucl. Phys. B* **480**, 341 (1996) [hep-ph/9606314].
- [19] D. Diakonov, In \*Peniscola 1997, Advanced school on non-perturbative quantum field physics\* 1-55 [hep-ph/9802298].
- [20] H. Mineo, W. Bentz and K. Yazaki, *Phys. Rev. C* **60**, 065201 (1999) [nucl-th/9907043].
- [21] I. C. Cloët, W. Bentz and A. W. Thomas, *Phys. Lett. B* **621**, 246 (2005) [hep-ph/0504229].
- [22] I. C. Cloët, W. Bentz and A. W. Thomas, *Phys. Rev. Lett.* **95**, 052302 (2005) [nucl-th/0504019].
- [23] I. C. Cloët, W. Bentz and A. W. Thomas, *Phys. Lett. B* **659**, 214 (2008) [arXiv:0708.3246 [hep-ph]].
- [24] W. Bentz, I. C. Cloët, T. Ito, A. W. Thomas and K. Yazaki, *Prog. Part. Nucl. Phys.* **61**, 238 (2008) [arXiv:0711.0392 [nucl-th]].
- [25] H. H. Matevosyan, W. Bentz, I. C. Cloët and A. W. Thomas, *Phys. Rev. D* **85**, 014021 (2012) [arXiv:1111.1740 [hep-ph]].
- [26] I. C. Cloët, W. Bentz and A. W. Thomas, *Phys. Rev. C* **90**, no. 4, 045202 (2014) [arXiv:1405.5542 [nucl-th]].
- [27] T. M. Aliev, K. Azizi and M. Savci, *Phys. Lett. B* **723**, 145 (2013) [arXiv:1303.6798 [hep-ph]].
- [28] I. C. Cloët, G. Eichmann, B. El-Bennich, T. Klahn and C. D. Roberts, *Few Body Syst.* **46**, 1 (2009) doi:10.1007/s00601-009-0015-x [arXiv:0812.0416 [nucl-th]].
- [29] G. Eichmann, *Phys. Rev. D* **84**, 014014 (2011) doi:10.1103/PhysRevD.84.014014 [arXiv:1104.4505 [hep-ph]].
- [30] J. Segovia, I. C. Cloët, C. D. Roberts and S. M. Schmidt, *Few Body Syst.* **55**, 1185 (2014) doi:10.1007/s00601-014-0907-2, 10.1007/s00601-014-0908-1 [arXiv:1408.2919 [nucl-th]].
- [31] H. -W. Lin and K. Orginos, *Phys. Rev. D* **79**, 034507 (2009) [arXiv:0712.1214 [hep-lat]].
- [32] S. Durr, Z. Fodor, J. Frison, C. Hoelbling, R. Hoffmann, S. D. Katz, S. Krieg and T. Kurth *et al.*, *Science* **322**, 1224 (2008) [arXiv:0906.3599 [hep-lat]].
- [33] A. Walker-Loud, H. -W. Lin, D. G. Richards, R. G. Edwards, M. Engelhardt, G. T. Fleming, P. Hagler and B. Musch *et al.*, *Phys. Rev. D* **79**, 054502 (2009) [arXiv:0806.4549 [hep-lat]].
- [34] S. Aoki *et al.* [PACS-CS Collaboration], *Phys. Rev. D* **79**, 034503 (2009) [arXiv:0807.1661 [hep-lat]].
- [35] P. E. Shanahan, A. W. Thomas and R. D. Young, *Phys. Lett. B* **718**, 1148 (2013) [arXiv:1209.1892 [nucl-th]].
- [36] P. E. Shanahan, A. W. Thomas, K. Tsushima, R. D. Young and F. Myhrer, *Phys. Rev. Lett.* **110**, no. 20, 202001 (2013) [arXiv:1302.6300 [nucl-th]].
- [37] S. Borsanyi *et al.*, *Science* **347**, 1452 (2015) [arXiv:1406.4088 [hep-lat]].
- [38] P. E. Shanahan, A. W. Thomas, R. D. Young, J. M. Zanotti, R. Horsley, Y. Nakamura, D. Pleiter and P. E. L. Rakow *et al.*, *Phys. Rev. D* **90**, 034502 (2014) [arXiv:1403.1965 [hep-lat]].
- [39] P. E. Shanahan, A. W. Thomas, R. D. Young, J. M. Zanotti, R. Horsley, Y. Nakamura, D. Pleiter and P. E. L. Rakow *et al.*, *Phys. Rev. D* **89**, 074511 (2014) [arXiv:1401.5862 [hep-lat]].
- [40] A. Chodos, R. L. Jaffe, K. Johnson and C. B. Thorn, *Phys. Rev. D* **10**, 2599 (1974).
- [41] S. Theberge, A. W. Thomas and G. A. Miller, *Phys. Rev. D* **22**, 2838 (1980) [Erratum-ibid. *D* **23**, 2106 (1981)].
- [42] S. Theberge and A. W. Thomas, *Phys. Rev. D* **25**, 284 (1982).
- [43] F. Myhrer and Z. Xu, *Phys. Lett. B* **108**, 372 (1982).
- [44] K. Kubodera, Y. Kohyama, K. Oikawa and C. W. Kim, *Nucl. Phys. A* **439**, 695 (1985).

- [45] K. Tsushima, T. Yamaguchi, Y. Kohyama and K. Kubodera, Nucl. Phys. A **489**, 557 (1988).
- [46] T. Yamaguchi, K. Tsushima, Y. Kohyama and K. Kubodera, Nucl. Phys. A **500**, 429 (1989).
- [47] G. Wagner, A. J. Buchmann and A. Faessler, Phys. Rev. C **58**, 3666 (1998) [nucl-th/9809015].
- [48] C. Boros and A. W. Thomas, Phys. Rev. D **60**, 074017 (1999) [hep-ph/9902372].
- [49] A. W. Thomas and G. Krein, Phys. Lett. B **456**, 5 (1999) [nucl-th/9902013].
- [50] A. W. Thomas and G. Krein, Phys. Lett. B **481**, 21 (2000) [nucl-th/0004008].
- [51] S. D. Bass and A. W. Thomas, Phys. Lett. B **684**, 216 (2010) [arXiv:0912.1765 [hep-ph]].
- [52] A. Silva, D. Urbano and K. Goeke, Nucl. Phys. A **755**, 290 (2005).
- [53] G. Ramalho, K. Tsushima and A. W. Thomas, J. Phys. G **40**, 015102 (2013) [arXiv:1206.2207 [hep-ph]].
- [54] M. E. Carrillo-Serrano, I. C. Cloët and A. W. Thomas, Phys. Rev. C **90**, no. 6, 064316 (2014) [arXiv:1409.1653 [nucl-th]].
- [55] H. Sanchis-Alepuz and C. S. Fischer, Eur. Phys. J. A **52**, no. 2, 34 (2016) doi:10.1140/epja/i2016-16034-1 [arXiv:1512.00833 [hep-ph]].
- [56] R. D. Young and A. W. Thomas, Phys. Rev. D **81**, 014503 (2010) [arXiv:0901.3310 [hep-lat]].
- [57] Y. Nambu and G. Jona-Lasinio, Phys. Rev. **122**, 345 (1961).
- [58] Y. Nambu and G. Jona-Lasinio, Phys. Rev. **124**, 246 (1961).
- [59] M. E. Carrillo-Serrano, W. Bentz, I. C. Cloët and A. W. Thomas, Phys. Rev. C **92**, no. 1, 015212 (2015) [arXiv:1504.08119 [nucl-th]].
- [60] Y. Ninomiya, W. Bentz and I. C. Cloët, Phys. Rev. C **91**, no. 2, 025202 (2015) [arXiv:1406.7212 [nucl-th]].
- [61] S. P. Klevansky, Rev. Mod. Phys. **64**, 649 (1992).
- [62] T. Hatsuda and T. Kunihiro, Phys. Rept. **247**, 221 (1994) [hep-ph/9401310].
- [63] D. Ebert, T. Feldmann and H. Reinhardt, Phys. Lett. B **388**, 154 (1996) [hep-ph/9608223].
- [64] G. Hellstern, R. Alkofer and H. Reinhardt, Nucl. Phys. A **625**, 697 (1997) [hep-ph/9706551].
- [65] W. Bentz and A. W. Thomas, Nucl. Phys. A **696**, 138 (2001) [nucl-th/0105022].
- [66] I. R. Afnan and A. W. Thomas, Top. Curr. Phys. **2**, 1 (1977).
- [67] U. Vogl and W. Weise, Prog. Part. Nucl. Phys. **27**, 195 (1991).
- [68] N. Ishii, W. Bentz and K. Yazaki, Nucl. Phys. A **587**, 617 (1995).
- [69] N. Ishii, W. Bentz and K. Yazaki, Phys. Lett. B **301**, 165 (1993).
- [70] N. Ishii, W. Bentz and K. Yazaki, Phys. Lett. B **318**, 26 (1993).
- [71] A. Buck, R. Alkofer and H. Reinhardt, Phys. Lett. B **286**, 29 (1992).